Neural Computing and Applications (2019) 31:4253–4270
https://doi.org/10.1007/s00521-017-3330-z

ORIGINAL ARTICLE

An expert 2DOF fractional order fuzzy PID controller for nonlinear systems

Vijay Mohan[1] · Himanshu Chhabra[1] · Asha Rani[1] · Vijander Singh[1]

Received: 29 June 2017 / Accepted: 28 December 2017 / Published online: 17 January 2018

Abstract
This work presents a generic two-degree-of-freedom fractional order fuzzy PI-D (2DOF FOFPI-D) controller dedicated to a class of nonlinear systems. The control law for proposed scheme is derived from basic 2DOF fractional order PID controller in discrete domain. Expert intelligence is embedded in overall derived control law by utilizing formula-based fuzzy design methodology. The controller structure comprises of fractional order fuzzy PI (FOFPI) and fractional order derivative filter to handle multiple issues and provides flexibility in design and self-tuning control feature. Further, the proposed scheme is compared with its integer order counterpart and 2DOF PI-D controller for coupled nonlinear 2-link robotic arm in real operating environment. The parameters of designed controllers are optimally tuned using multi-objective non-dominated sorting genetic algorithm-II for attaining low variation in control effort and error index. Intensive simulation studies are performed to analyze trajectory tracking, model uncertainty, disturbance due to cogging, sensor noise and noise as well as disturbance rejection simultaneously. Results demonstrate the superior performance of 2DOF FOFPI-D controller as compared to other designed controllers in the facets of different operating conditions.

Keywords 2DOF FOFPI-D · Formula-based fuzzy design · Multi-objective optimization · Robustness testing

1 Introduction

Expert system and its applications have risen to a great level over the last few decades with the advent of artificial intelligence. Various fields like industrial automation, robotics, bio-metric recognition and machine learning have well utilized the potential of artificial intelligence. The use of intelligent techniques such as fuzzy logic and neural network has made the automation more effective and efficient by incorporating human decision capability to expert system. Most of the automation systems usually exhibit nonlinearity and uncertainty and also suffer from disturbance and internal or external noise. So, there is a need for intelligent expert solution for smooth and efficient functioning of such systems. Conventional controllers, such as proportional–integral–derivative (PID) controller, fail to deliver efficient control for systems with nonlinear and uncertain dynamics [1]. However, till date 90% of the controllers used in industry are PID because of its many advantages such as cost-effectiveness, ease of installation and operation [2]. Therefore, researchers across the globe are more inclined to enhance the capabilities of PI/PD/PID controllers by merging artificial intelligence with basic conventional structure. Several examples of such hybrid fuzzy controllers are available in the literature, which are quite effective and robust [3–13].

The performance of expert fuzzy controllers is further improved by the introduction of fractional calculus as it provides extra degree of freedom and flexibility to design scheme. In these controllers, the order of integration and differentiation is generalized to non-integer values. Diverse applications of fractional order fuzzy controllers are seen in the literature. Kumar and Kumar [14] designed a fractional order (FO) fuzzy pre-compensated FOPID controller for robotic manipulator. The controller parameters are optimized using hybrid artificial bee colony-genetic algorithm (ABC-GA) for minimizing ITAE. Simulation results prove better performance of proposed

✉ Vijay Mohan
vijay.mohan@nsit.ac.in; vijay13787@gmail.com

[1] Division of Instrumentation and Control Engineering, Netaji Subhas Institute of Technology, University Of Delhi, New Delhi 110078, India

controller as compared to integer order fuzzy pre-compensated PID, fuzzy PID and PID control scheme in various case studies. The authors [15] also proposed a family of interval type-2 fractional order fuzzy PID controllers, and their performance is evaluated on fractional order systems. The design variables of the controllers are optimized using ABC-GA technique. Simulation results illustrate the effectiveness of these controllers in terms of disturbance rejection, uncertainty, low variation in control signal and better tracking. Sharma et al. [16] designed a new two-layered fractional order fuzzy logic control technique for two-link robot. Performance of the designed controller is compared with single-layer fuzzy logic controller and traditional PID. Optimum parameters of the controllers are achieved using cuckoo search algorithm. Results prove that proposed control scheme outruns the other controllers in all aspects. Das et al. [17] presented different structures of fractional order fuzzy PID to control fractional order system having dead time. Non-integer operators and scaling gains of the controllers are optimally tuned using genetic algorithm, and performance is compared quantitatively for different case studies. The authors [18] also performed comparative study of fractional order fuzzy PID and its integer order variant for delayed nonlinear and open-loop unstable process. The parameters of controllers are optimized using real-coded genetic algorithm, and the performance of FO fuzzy PID is found superior over fuzzy PID. Kumar et al. [19] presented fractional order fuzzy PD for controlling active suspension system to achieve comfortable ride. The performance of designed controller is compared with its integer order counterpart for uncertain environment with different road profiles. It is found that FO-FPD outperforms FPD in every aspect. Jesus et al. [20] designed a genetic algorithm tuned fractional order fuzzy PD plus conventional integral controller. The effectiveness of controller is proved by considering different examples. The expert fractional order fuzzy controllers offer robust and effective control. Therefore, these controllers are applied in different fields such as combined cycle power plant [21], smart base-isolated structures [22], financial system [23], hybrid power plant [24], robotic system [25, 26], nuclear reactor [27], distillation column [28] and hybrid electric vehicle [29].

The degree of freedom of a controller signifies the number of closed loops that can be modified individually and plays a significant role in designing an efficient control strategy. A 1-DOF controller has only one closed loop, and hence, it is incapable of addressing multiple conflicting issues, i.e., trajectory tracking and disturbance rejection simultaneously [30]. Both conventional and hybrid fuzzy controllers are 1-DOF in nature and thus do not provide solution to such problems [2, 30, 31]. The control problems most frequently are coupled in nature and have several conflicting objectives. The recent research in this field demonstrates that 2DOF controller provides a good solution to these problems. As an illustration, Pachauri et al. [32] presented 2DOF PID-based inferential control of bioreactor. The suggested controller outperforms the PID in closed-loop control for set-point tracking, disturbance rejection and noise suppression. Ghosh et al. [33] also proved that 2DOF PID outperforms the 1DOF PID for magnetic levitation system. Richa et al. [31] compared the performance of CSA tuned 2DOF FOPID, 2DOF PID and PID for robotic manipulator, and results proved the superiority of 2DOF FOPID over other implemented controllers. Debbarma et al. [34] presented the comparative study of firefly tuned 2DOF FOPID, 2DOF PID, PID and PI controllers for AGC of power system. Simulation results claimed that 2DOF FOPID performs significantly better in all aspects over other controllers. Li et al. [35] overcome the problem of coupled robustness and dynamic response in 1DOF FOPID for fractional order system with dead time by utilizing internal model control-based 2DOF FOPID. The simple design and tuning approach of the proposed controller proves its effectiveness over 1DOF FOPID controller. Different structures of expert 2DOF fuzzy PI controller are applied to a laboratory DC drive by Precup et al. [2]. Experimental results claim that the performance of generic 2DOF fuzzy PI control structures is superior to 2DOF PI controller.

It is evident from the literature that amalgamation of fractional calculus with 2DOF PID enhances its performance. Further embedding artificial intelligence to conventional controller leads to an expert system with increased efficiency. This motivated us to design a new generic two-degree-of-freedom fractional order fuzzy proportional integral minus derivative (2DOF FOFPI-D) controller which explores the advantages of formula-based fuzzy in association with 2DOF fractional order PID structure. The structure of controller comprises of serial compensator (FOFPI) and fractional order derivative filter (FODF) to handle multiple issues simultaneously. The proposed scheme is adaptive in nature, as the gains of serial compensator are nonlinear functions of error and fractional rate of error. Further, the performance of designed controller is assessed by comparing it with 2DOF fuzzy PI-D (2DOF FPI-D) and 2DOF PI-D for coupled, nonlinear and complex two-link robotic arm in servo and regulatory modes. Fractional operators increase the flexibility of controllers at the cost of higher number of design variables, thereby making it difficult to tune. Thus, the design variables of each controller are tuned optimally using non-dominated sorting genetic algorithm-II [36] so that error index and variations in control are small. The performance of designed controllers is

examined by conducting comprehensive simulation study on the basis of integral absolute error (IAE). The benefit of proposed scheme is that it incorporates simple formula-based fuzzy, wherein inputs are fuzzified using two triangular membership functions. This leads to only four if–then rules [4]. Another merit of the control scheme is that it is generic as its design does not require the model of system. Moreover, it also enjoys the benefits of 2DOF structure along with flexibility in design due to fractional operators. The key contributions of this work can be summarized as follows:

- In this paper, a fractional order formula-based intelligent control technique, namely 2DOF FOFPI-D, is proposed. Its control law is derived analytically using linear 2DOF FOPID technique in discrete domain. Further formula-based fuzzy design methodology is incorporated in derived control law to provide expert intelligence and self-tuning control feature.
- The proposed 2DOF FOFPI-D controller is found to be more efficient and robust in virtually created real operating environment by considering issues such as parametric uncertainty, actuator disturbance and measurement noise as compared to 2DOF fuzzy PI-D (2DOF FPI-D) and 2DOF PI-D.
- The benefits of proposed controller make it appropriate for real-time control applications [31, 32] such as robotic arm, distillation column, bioreactor, flexible link and joint robot.

After a brief literature review in Sect. 1, the design approach of 2DOF FOFPI-D controller is presented in Sect. 2. In Sect. 3, introduction and design steps of NSGA-II algorithm are outlined. The mathematical model of robotic manipulator under consideration is given in Sect. 4. Section 5 analyzes the simulation results of 2DOF FOFPI-D and other controllers for two-link robotic arm. The discussion of results is presented in Sect. 6. Finally concluding remarks regarding significance and impact of the research work are discussed in Sect. 7.

2 Design of adaptive 2DOF FOFPI-D controller

The aim of this work is to devise an adaptive control scheme for nonlinear systems, which provides accurate control with minimum control effort while addressing several conflicting issues. The analytical formulae for proposed control scheme are derived from conventional 2DOF FOPID controller. The formula-based fuzzy design is then embedded in derived control law, which makes it intelligent and adaptive.

2.1 Mathematical formulation of 2DOF FOFPI-D control law

The general equation of control action for classical 2DOF PID controller in frequency domain is expressed as follows [30]:

$$U_{\text{2DOF PID}} = P(b*R-Y) + \frac{I}{s}(R-Y) + \frac{K_{\text{D}}N}{1+\frac{N}{s}}(c*R-Y) \quad (1)$$

The 2DOF fractional order PID (2DOF FOPID) for non-integer order of integration and differentiation is represented as:

$$U_{\text{2DOF FOPID}} = P(b*R-Y) + \frac{I}{s^{\lambda}}(R-Y) + \frac{K_{\text{D}}N}{1+\frac{N}{s^{\mu}}}(c*R-Y) \quad (2)$$

where P, I and K_{D} are proportional, integral and derivative gains, respectively. R is reference signal and Y is the output of nonlinear system. b and c are weights of 2DOF controller, whereas λ and μ are orders of fractional operator. N and s are the filter coefficient and complex frequency, respectively.

A large spike or kick is observed in derivative control action due to discontinuous or sudden changes in reference signal. In practical applications, the control signal drives final control element such as valve, electric actuators and fluid couplings. The large spikes in control signal may damage the element [37]. Typically derivative action for abrupt changes in reference is undesirable and is required only for system response Y. Therefore, the control law '$U_{\text{2DOF FOPID}}$' is modified by considering the weight 'c' to be zero, so that derivative action depends only on system output 'Y'. The derivative kick is thus completely avoided, and Eq. (2) is modified as:

$$U_{\text{2DOF FOPI-D}} = \underbrace{\left(Pb+\frac{I}{s^{\lambda}}\right)E(s)}_{U_{\text{sc}}} - \underbrace{\left(\frac{K_{\text{D}}N}{1+\frac{N}{s^{\mu}}}+P(1-b)\right)Y(s)}_{U_{\text{ff}}} \quad (3)$$

where $U_{\text{sc}} = \left(Pb+\frac{I}{s^{\lambda}}\right)E(s)$, $U_{\text{ff}} = \left(\frac{K_{\text{D}}N}{1+\frac{N}{s^{\mu}}}+P(1-b)\right)Y(s)$ and $E(s) = R(s) - Y(s)$ is error. The control law (Eq. 3) for two-degree-of-freedom fractional order proportional plus integral minus derivative controller comprises of a serial compensator 'U_{sc}' and fractional order derivative filter (FODF) 'U_{ff}'. The serial compensator is equivalent to fractional order proportional–integral (FOPI) controller, where proportional action improves the response time of system by decreasing the time constant and integral action reduces the steady-state error [38]. Therefore, it improves

transient as well as steady-state response of the system. Generally high-frequency sensor noise affects the system output, and conventional derivative term may produce unwanted large control action. This problem is solved by putting a fractional order filter with derivative term which attenuates the noise and limits the derivative action [39]. Hence, FOFD possesses predictive capability while eliminating the chattering of high-frequency noise. Further the conventional FOPI controller is replaced by fractional order fuzzy PI controller leading to a novel two-degree-of-freedom fractional order fuzzy proportional plus integral minus derivative controller. The controller is designed using analytical formulae to provide self-tuning control ability besides preserving the properties of traditional controller [12]. Analytical formulae for transforming the serial compensator to FO fuzzy PI controller are derived as:

$$U_{\mathrm{sc}}(s) = \left\{ Pb + \frac{I}{s^{\lambda}} \right\} E(s) \tag{4}$$

Using backward transformation $s = \frac{(1-z^{-1})}{T}$, where $T > 0$ is sampling time. Further Eq. (4) is transformed into discrete form as:

$$\begin{aligned} U_{\mathrm{sc}}(z) &= \left\{ Pb + \frac{IT^{\lambda}}{(1-z^{-1})^{\lambda}} \right\} E(z) \\ \Delta U_{\mathrm{sc}}(z) &= \left\{ Pb \left(\frac{1-z^{-1}}{T} \right)^{\lambda} + I \right\} E(z) \end{aligned} \tag{5}$$

where

$$\Delta U_{\mathrm{sc}}(z) = U_{\mathrm{sc}}(z) \left(\frac{1-z^{-1}}{T} \right)^{\lambda} \tag{6}$$

Expanding Eq. (5) using power series expansion [40] as

$$\Delta U_{\mathrm{sc}}(z) = \frac{Pb}{T^{\lambda}} \sum_{k=0}^{\infty} (-1)^k \binom{\lambda}{k} z^{-k} E(z) + IE(z) \tag{7}$$

Taking inverse Z-transform of Eq. (7), it yields

$$\Delta u_{\mathrm{sc}}(nT) = \frac{Pb}{T^{\lambda}} \sum_{k=0}^{\infty} (-1)^k \binom{\lambda}{k} e((n-k)T) + Ie(nT) \tag{8}$$

The first term on the right side of Eq. (8) is similar to the formulation specified by Lubich for non-integer derivative/integral of order α for an arbitrary function $x(nT)$ [41] and is expressed as:

$$D^{\mp\alpha} x(nT) = T^{\pm\alpha} \sum_{k=0}^{\infty} (-1)^k \binom{\mp\alpha}{k} x((n-k)T) \tag{9}$$

Equating Eqs. (8) and (9), it yields

$$\Delta u_{\mathrm{sc}}(nT) = PbD^{\lambda} e(nT) + Ie(nT)$$

Explicitly

$$\Delta u_{\mathrm{sc}}(nT) = K_P e(nT) + K_I e_{\mathrm{r}}(nT) \tag{10}$$

where $K_P = I$, $K_I = Pb$, $e_{\mathrm{r}}(nT) = D^{\lambda} e(nT)$ and $e(nT) = r(nT) - y(nT)$. Similarly, solving Eq. (6) for control law gives

$$\begin{aligned} U_{\mathrm{sc}}(z) &= T^{\lambda} \sum_{k=0}^{\infty} (-1)^k \binom{-\lambda}{k} z^{-k} \Delta U_{\mathrm{sc}}(z) \\ u_{\mathrm{sc}}(nT) &= T^{\lambda} \sum_{k=0}^{\infty} (-1)^k \binom{-\lambda}{k} \Delta u_{\mathrm{sc}}(nT) \\ u_{\mathrm{sc}}(nT) &= D^{-\lambda} (\Delta u_{\mathrm{sc}}(nT)). \end{aligned} \tag{11}$$

Equation (11) is transformed to fuzzy control action by multiplying right-hand side with scaling gain K_u as

$$u_{\mathrm{sc}}(nT) = K_u D^{-\lambda} (\Delta u_{\mathrm{sc}}(nT)) \tag{12}$$

Thus, overall control action of 2DOF FOFPI-D is expressed as:

$$\begin{aligned} u_{\mathrm{2DOFFOFPI-D}} &= u_{\mathrm{sc}} - u_{\mathrm{ff}} \\ u_{\mathrm{2DOFFOFPI-D}} &= K_u D^{-\lambda} (\Delta u_{\mathrm{sc}}(nT)) \\ &\quad - \left\{ \frac{K_D N D^{\mu}}{D^{\mu} + N} + P(1-b) \right\} y(nT) \end{aligned} \tag{13}$$

The generalized structure of 2DOF FOFPI-D (Eqs. 10, 13) for nonlinear system is shown in Fig. 1.

2.2 Framework for fuzzy control

Standard fuzzy design methodology, which includes fuzzification, control rule and defuzzification, is embedded to analytical formula derived in the last section.

2.2.1 Fuzzification

The inputs and output of serial compensator are fuzzified separately, and control rules are designed using Eq. (11). Serial compensator employs two inputs: error $\tilde{e}(nT) = K_{\mathrm{P}} e(nT)$ and fractional rate of error $\tilde{e}_{\mathrm{r}}(nT) = K_{\mathrm{I}} e_{\mathrm{r}}(nT)$. Two triangular membership functions, *n*: negative and *p*: positive, are selected for both inputs. On the other hand, output $\Delta u_{\mathrm{sc}}(nT)$ is fuzzified using four singleton membership functions, *nl*: negative large, *ns*: negative small, *ps*: positive small and *pl*: positive large. Corresponding input and output membership functions of serial compensator are shown in Fig. 2. The constant $L > 0$ is determined using NSGA-II optimization.

2.2.2 Control rule base

The control rule base plays a key role in designing an efficient fuzzy logic controller. These rules are framed

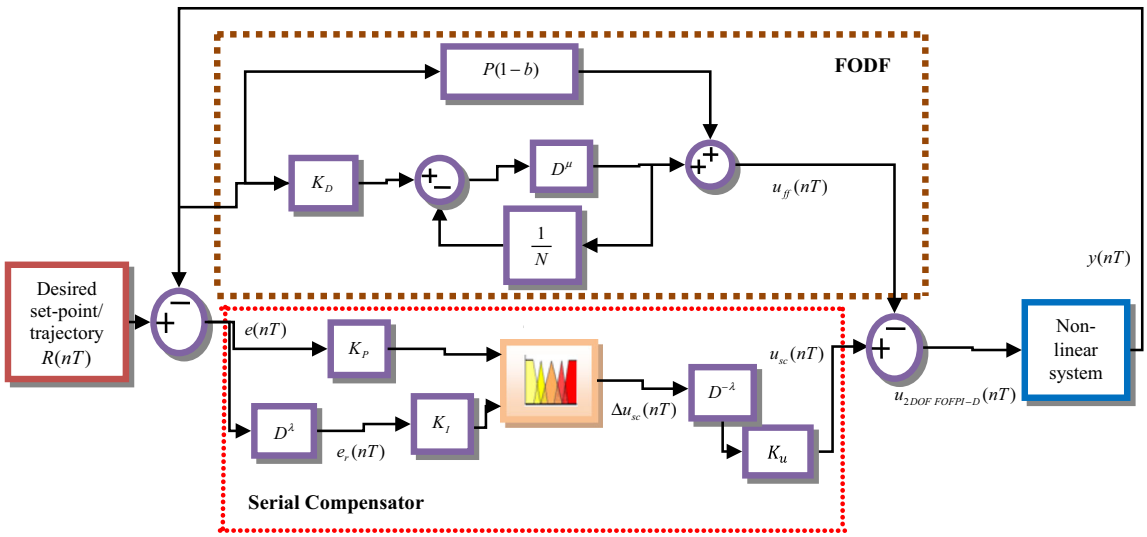

Fig. 1 Control structure of generic two-degree-of-freedom fractional order fuzzy PI-D for nonlinear system

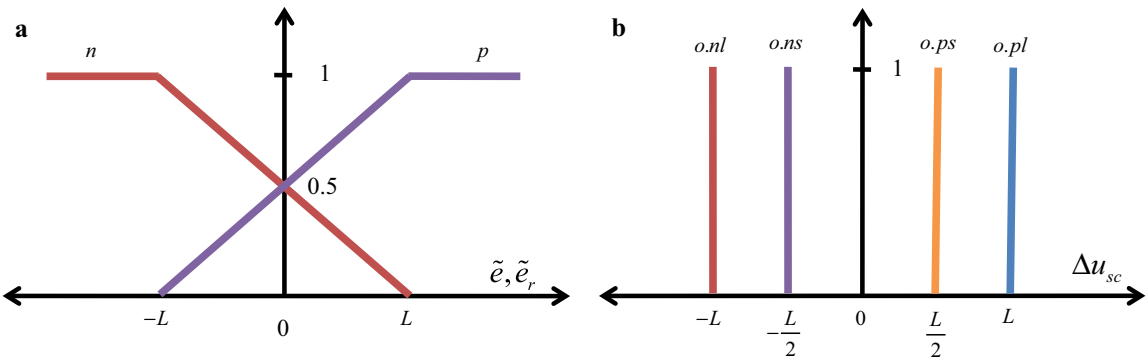

Fig. 2 Membership functions of serial compensator **a** input and **b** output

either on the basis of operator experience or knowledge of control system dynamics. In this work, four rules for serial compensators are designed on the basis of control system knowledge. The following control rules are designed for serial compensator on the basis of input and output membership function as follows:

$$(R^1):\ \text{If } \tilde{e} = \tilde{e}\cdot n \text{ and } \tilde{e}_{\mathrm{r}} = \tilde{e}_{\mathrm{r}}\cdot n \text{ then } \Delta u_{\mathrm{sc}} = o\cdot nl$$

$$(R^2):\ \text{If } \tilde{e} = \tilde{e}\cdot n \text{ and } \tilde{e}_{\mathrm{r}} = \tilde{e}_{\mathrm{r}}\cdot p \text{ then } \Delta u_{\mathrm{sc}} = o\cdot ns$$

$$(R^3):\ \text{If } \tilde{e} = \tilde{e}\cdot p \text{ and } \tilde{e}_{\mathrm{r}} = \tilde{e}_{\mathrm{r}}\cdot n \text{ then } \Delta u_{\mathrm{sc}} = o\cdot ps$$

$$(R^4):\ \text{If } \tilde{e} = \tilde{e}\cdot p \text{ and } \tilde{e}_{\mathrm{r}} = \tilde{e}_{\mathrm{r}}\cdot p \text{ then } \Delta u_{\mathrm{sc}} = o\cdot pl$$

where $\tilde{e} = K_P e = K_P(r-y)$ is error, $\tilde{e}_{\mathrm{r}} = K_I e_{\mathrm{r}}(nT) = K_I\left(D^{\lambda}r - D^{\lambda}y\right)$ is the fractional rate of error and Δu_{sc} is fuzzy control action of serial compensator. Also, '$\tilde{e}\cdot p$' signifies error positive, '$\tilde{e}_r\cdot n$' means fractional rate of error negative and '$o\cdot ns$' is output negative small and so on. A set of four rules decides the fuzzy control action of serial compensator, and their formulation is described as:

In rule 1 (R^1), $\tilde{e}\cdot n$ (error negative) simply means that system response $y(nT)$ is above the reference signal $r(nT)$ and corresponding '$\tilde{e}_r\cdot n$' fractional rate of error negative ($D^{\lambda}y > D^{\lambda}r$) implies that response is moving up at a rate faster than reference from previous instant. Explicitly from rule 1, the response is above and moving up at faster rate than reference. Therefore to bring down the response y close to reference, the fuzzy control action of serial compensator Δu_{sc} is set as negative large. In rule 2(R^2), the response of system is above reference but moving down at faster pace than desired trajectory. So, Δu_{sc} is set as negative small. Similarly, rules R^3 and R^4 can be explained.

2.2.3 Defuzzification

The control action of serial compensator is defuzzified by center-of-mass formula [4]. The mathematical expression for defuzzified control action Δu_{sc} is expressed as:

$$\Delta u_{sc} = \frac{\sum(\text{output corresponding to membership value of input} * \text{membership value of input})}{\sum \text{membership value of input}} \tag{14}$$

The control action of serial compensator is defuzzified by decomposing inputs $\tilde{e}$ and $\tilde{e}_r$ in 20 input combination (IC) regions as shown in Fig. 3. The 2-dimensional picture is obtained by plotting membership function of $\tilde{e}$ and $\tilde{e}_r$ on horizontal and vertical axis, respectively. The rules R^1 to R^4 and membership functions along with IC regions are used to estimate the defuzzified control action 'Δu_{sc}'. Now, let $\tilde{e}$ and $\tilde{e}_r$ fall in region IC1. It is clear from Fig. 3 that range of $\tilde{e}$ and $\tilde{e}_r$ is $[0, L]$ and $[-L, 0]$, respectively. Also, it is observed from Fig. 2a that value of $\tilde{e} \cdot n < 0.5$ and $\tilde{e}_r \cdot n > 0.5$. Therefore, rule R^1 and Zadeh's logic [42] collectively yield the following:

IF $\tilde{e} = \tilde{e}.n$ AND $\tilde{e}_r = \tilde{e}_r \cdot n$ implies minimum $\{\tilde{e} \cdot n, \tilde{e}_r \cdot n\} = \tilde{e} \cdot n$

Therefore, for rule 1

$$R^1 \begin{cases} \text{corresponding input membership value is } \tilde{e} \cdot n \\ \text{membership value of output is } o \cdot \text{nl} \end{cases}$$

Likewise, other rules and Zadeh's logic in IC1 lead to

$$R^2 \begin{cases} \text{corresponding input membership value is } \tilde{e} \cdot n \\ \text{membership value of output is } o \cdot ns \end{cases}$$

$$R^3 \begin{cases} \text{corresponding input membership value is } \tilde{e}_r \cdot n \\ \text{membership value of output is } o \cdot ps \end{cases}$$

$$R^4 \begin{cases} \text{corresponding input membership value is } \tilde{e}_r \cdot p \\ \text{membership value of output is } o \cdot pl \end{cases}$$

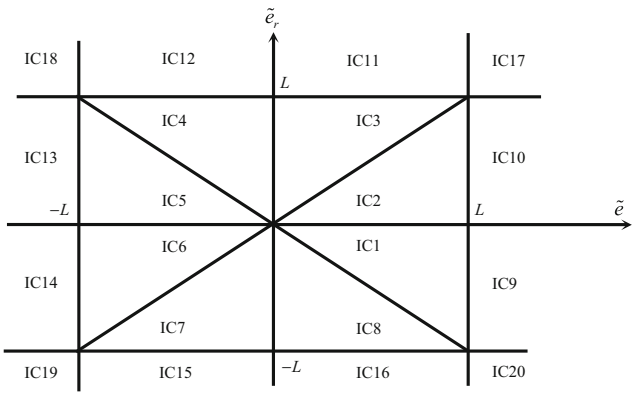

Fig. 3 Input combination region for serial compensator

It can be easily verified that above rules are true for region IC2. Therefore, in regions IC1 and IC2 the defuzzification formula gives:

$$\Delta u_{sc} = \frac{o \cdot nl * \tilde{e} \cdot n + o \cdot ns * \tilde{e} \cdot n + o \cdot ps * \tilde{e}_r \cdot n + o \cdot pl * \tilde{e}_r \cdot p}{\tilde{e} \cdot n + \tilde{e} \cdot n + \tilde{e}_r \cdot n + \tilde{e}_r \cdot p} \tag{15}$$

Now, mathematical representations of input membership functions are derived from the straight-line formula [4, 9], given as

$$\tilde{e} \cdot p = \frac{K_P e(nT) + L}{2L}, \quad \tilde{e} \cdot n = \frac{-K_P e(nT) + L}{2L}$$
$$\tilde{e}_r \cdot p = \frac{K_I e_r(nT) + L}{2L}, \quad \tilde{e}_r \cdot n = \frac{-K_I e_r(nT) + L}{2L}$$

Now, substituting the above formulae and $o \cdot pl = L$, $o \cdot ps = \frac{L}{2}$, $o \cdot nl = -L$, $o \cdot ns = -\frac{L}{2}$ in Eq. (15), the output $\Delta u_{sc}(nT)$ in regions IC1 and IC2 is expressed as:

$$\Delta u_{sc}(nT) = \frac{L}{4(2L - K_P e(nT))}[3K_P e(nT) + K_I e_r(nT)]$$

In regions IC1 and IC2, $\tilde{e}(nT) \geq 0$. Likewise, Δu_{sc} in regions IC5 and IC6 is expressed as:

$$\Delta u_{sc}(nT) = \frac{L}{4(2L + K_P e(nT))}[3K_P e(nT) + K_I e_r(nT)]$$

The value of $\tilde{e}(nT) \leq 0$ for regions IC5 and IC6. Therefore, combined formula for regions IC1, IC2, IC5 and IC6 is as follows:

$$\Delta u_{sc}(nT) = \frac{L(3K_P e(nT) + K_I e_r(nT))}{4(2L - K_P|e(nT)|)}$$

Explicitly

$$\Delta u_{sc}(nT) = \left[\frac{3LK_P}{4(2L - K_P|e(nT)|)}\right] e(nT) + \left[\frac{LK_I}{4(2L - K_P|e(nT)|)}\right] e_r(nT) \tag{16}$$

The above formula of control action has structure similar to conventional FOPD controller with nonlinear gains, thereby providing self-tuning feature to the controller [12]. These variable gains play a vital role in improving the performance of controller. An increase in $e(nT)$ decreases $2L - K_P|e(nT)|$, which in turn increases the overall gains

Table 1 Formulae for $\Delta u_{sc}(nT)$ in all regions of IC

IC regions	FOFPI output (Δu_{sc})
IC 1, 2, 5, 6	$\frac{L(3K_P e(nT)+K_I e_r(nT))}{4(2L-K_P\|e(nT)\|)}$
IC 3, 4, 7, 8	$\frac{L(3K_P e(nT)+K_I e_r(nT))}{4(2L-K_I\|e_r(nT)\|)}$
IC 9,10	$\frac{1}{4}(3L+K_I e_r(nT))$
IC 11,12	$\frac{1}{4}(3L+K_P e(nT))$
IC 13,14	$\frac{1}{4}(K_I e_r(nT)-3L)$
IC 15,16	$\frac{1}{4}(K_P e(nT)-3L)$
IC 17	L
IC 18	$-L/2$
IC 19	$-L$
IC 20	$L/2$

of 'Δu_{sc}' and vice versa. Thus, controller generates small corrective action when error diminishes but as soon as error increases, controller takes large corrective action. In the similar manner, control action of serial compensator for remaining IC regions is acquired and listed in Table 1. The brief summary of design procedure to acquire the control structure is outlined as follows:

1. Initially basic 2DOF fractional order PID controller is split into FOPI and FODF component in discrete domain.
2. Fuzzy expertise is incorporated in FOPI component (Eq. 10) by fuzzifying independent (input) variables $K_P e(nT)$ and $K_I e_r(nT)$ by simple triangular membership functions and the dependent (output) variable $\Delta u_{sc}(nT)$ by singleton membership functions.
3. The rule base is framed to map input–output membership functions on the basis of system knowledge.
4. Fuzzified output $\Delta u_{sc}(nT)$ is converted into crisp value using center-of-mass defuzzification algorithm. The defuzzified output is fractionally integrated and scaled by gain K_u to generate serial compensator output $u_{sc}(nT)$ (Eq. 12).
5. The overall control action of proposed controller is obtained by algebraically adding the outputs of serial compensator and fractional order derivative filter given in Eq. (13).

Further, designed 2DOF FOFPI-D controller is transformed to its integer order equivalent (2DOF FPI-D) by considering the values of fractional order λ and μ to be 1.

2.3 Implementation of fractional order operators

Over the last few decades, there has been a significant use of fractional calculus in the field of control system, filter design, system modeling and image processing [17, 25, 43, 44]. To implement fractional order operator, numerous methods are reported in the literature [45, 46]. In this work, fractional differentiator/integrator in discrete domain is designed by binomially [40] expanding backward difference transformation in operator $s^{\pm\alpha}$ as

$$s^{\pm\alpha} = \left(\frac{1-z^{-1}}{T}\right)^{\pm\alpha} \tag{17}$$

$$s^{\pm\alpha} = T^{\mp\alpha}\sum_{i=0}^{\infty}(-1)^i\frac{(\pm\alpha)(\pm\alpha-1)(\pm\alpha-2)\cdots(\pm\alpha-i+1)}{i!}z^{-i} \tag{18}$$

Denoting discrete-time differentiator and integrator operator with D, thus

$$D^{\pm\alpha}(z^{-1}) = T^{\mp\alpha}\sum_{i=0}^{\infty}(-1)^i\binom{\pm\alpha}{i}z^{-i} \text{ where } \binom{\pm\alpha}{i} = \frac{(\pm\alpha)(\pm\alpha-1)(\pm\alpha-2)\cdots(\pm\alpha-i+1)}{i!}$$

Therefore, differentiation and integration [41] of discrete-time arbitrary function $x(nT)$, which is equivalent to well-known Grunwald–Letnikov [47], are represented as:

$$D^{\pm\alpha}x(nT) = T^{\mp\alpha}\sum_{i=0}^{\infty}(-1)^i\binom{\pm\alpha}{i}x((n-i)T) \tag{19}$$

Realization of Eq. (19) requires computation of infinite number of coefficients and delay units. Therefore, to design practically feasible fractional order operator, principle of short memory is utilized as:

$$D^{\pm\alpha}x(nT) = T^{\mp\alpha}\sum_{i=0}^{M}(-1)^i\binom{\pm\alpha}{i}x((n-i)T) \tag{20}$$

where α is the order of operator, T is sampling time and M is number of delay elements to generate last few samples and its value is chosen as 100.

3 Multi-objective non-dominated sorting genetic algorithm-II

The metaheuristic algorithms are generally single objective in nature. Their primary aim is to discover best solution by optimizing the fitness function that lumps many objectives into one. These objectives are usually clashing and contradictory with each other, and many a times optimization of one objective, results into compromise of other objectives. Moreover, optimization by weighted sum of objectives provides a single optimum solution, and therefore, designer has no choice to trade objectives against each other according to the requirements. Another issue is to determine exact and accurate value of weights, which suits

designer's preferences, as slightest change in weights results in completely different solutions. These shortcomings may be overcome by a multi-objective algorithm, which provides a bunch of solutions instead of single best solution, thus giving the designer freedom to choose suitable final optimum solution.

NSGA-II is broadly used multi-objective optimization algorithm because of its simple population-based search approach, which is suitable for diverse fields of engineering. The Pareto-based methodology of NSGA-II has been widely utilized for contradictory multi-objective problems because of it is simple, direct and efficient non-dominant positioning technique, which results in various levels of Pareto fronts [48–51]. Further researchers have validated that NSGA-II has a superior sorting plan and consolidates elitism component as compared to NSGA-I [36]. In this work, the essential necessity is minimization of position error with least variation in control action. Therefore, objective functions [50] considered can be mathematically expressed as:

$$f_1 = \sum|\theta_{d_1}(nT) - \theta_1(nT)| + \sum|\theta_{d_2}(nT) - \theta_2(nT)| \tag{21}$$

$$f_2 = \sum|\tau_1(nT+T) - \tau_1(nT)| + \sum|\tau_2(nT+T) - \tau_2(nT)| \tag{22}$$

The objective functions attempt accurate position tracking with fairly small control effort. But these objectives are contradictory and at odds with each other (i.e., reducing variation in control effort results in increased tracking error and vice versa). Therefore, both objectives f_1 and f_2 need to be minimized simultaneously for efficient functioning of control loop. Steps for implementing NSGA-II algorithm are briefly outlined as:

(a) Initialize consistently distributed parent population of size P on the basis of parent's range.
(b) Evaluate the objectives for individuals and sort the population based on non-domination.
(c) Allot each result a rank equivalent to its non-domination level.
(d) Use the standard binary tournament selection method.
(e) Utilize the simulated binary crossover and polynomial mutation to make a posterity population of size P.
(f) Merge the parent and posterity population to create broadened population of size 2P.
(g) Sort the broadened population on the basis of non-domination.
(h) Fill new population of size P with the entities from the sorting fronts beginning from the best.
(i) The crowding-distance method is used to assure diversity, if a front can only partially fill the subsequent generation. The crowding-distance method keeps up variety in the population and avoids convergence to local optimum solution.
(j) Repeat steps (b)–(i) until a stopping condition is encountered.

The parameters of 2DOF FOFPI-D, its integer order counterpart and 2DOF PI-D are optimized using NSGA-II. The designed controllers are tested on highly nonlinear two-link robotic manipulator for trajectory tracking, model uncertainty, disturbance and noise rejection.

4 Dynamics of two-link robot

Robotic manipulators are of keen interest to control engineers because of highly complex, nonlinear and coupled dynamics. The tight position tracking of end-effector for such complex system is a challenging task for the experts. Robotic manipulator is an integral part of numerous industries like process, automation, chemical, nuclear power plant, space application and medical sciences for the purpose of pick and place, precision surgeries, cutting, grinding, drilling and assembly. The mechanical model of robotic manipulator under consideration is shown in Fig. 4. It consists of two links having length l_1 and l_2 with their center of mass m_1 and m_2 lying at distal ends of links, respectively. DC motors are attached at points A and B to provide controlling torque, whereas encoders are used to estimate the angular position (θ_1 and θ_2) and velocity ($\dot{\theta}_1$ and $\dot{\theta}_2$) of the links. The descriptions of related variable of the manipulator with their nominal values are listed in Table 2. The dynamics of two-link robotic manipulator is described [52] below

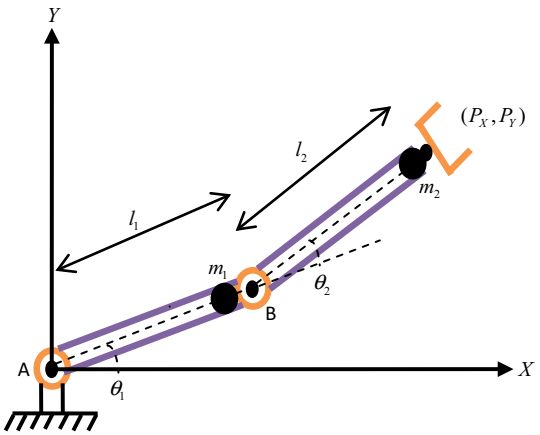

Fig. 4 Model of robotic manipulator

Table 2 Description of variables with their nominal values [50]

Description	Symbols	Nominal value	SI units
Center-of-mass link-1	m_1	0.1	Kg
Center-of-mass link-2	m_2	0.1	Kg
Length of link-1	l_1	0.8	m
Length of link-2	l_2	0.4	m
Acceleration due to gravity	g	9.81	m/s^2
Position of link-1 and link-2	θ_1 and θ_2	–	rad
Torque of link-1 and link-2	τ_1 and τ_2	–	Nm

where parameters of link-1 and link-2 are symbolized by subscripts 1 and 2, respectively.

$$\begin{aligned}\tau_1 = {} & m_2 l_2^2(\ddot{\theta}_1 + \ddot{\theta}_2) + (m_1 + m_2) l_1^2 \ddot{\theta}_1 \\ & + m_2 l_1 l_2 \cos\theta_2 (2\ddot{\theta}_1 + \ddot{\theta}_2) - m_2 l_1 l_2 \sin\theta_2 (\dot{\theta}_2^2) \\ & - 2 m_2 l_1 l_2 \sin\theta_2 \dot{\theta}_1 \dot{\theta}_2 + (m_1 + m_2) l_1 g \cos\theta_1 \\ & + m_2 l_2 g \cos(\theta_1 + \theta_2)\end{aligned} \tag{23}$$

$$\begin{aligned}\tau_2 = {} & m_2 l_1 l_2 \cos\theta_2 \ddot{\theta}_1 + m_2 l_2 g \cos(\theta_1 + \theta_2) \\ & + m_2 l_2^2 \left(\ddot{\theta}_1 + \ddot{\theta}_2\right) + m_2 l_1 l_2 \sin\theta_2 \dot{\theta}_1^2\end{aligned} \tag{24}$$

The control schemes derived in Sect. 2 are tested on the two-link robotic manipulator. The results obtained are discussed in the next section.

5 Results

This work presents an expert solution for nonlinear systems where multiple issues need to be addressed. A new 2DOF FOFPI-D controller is proposed for the purpose. The controller possesses the benefits of 2DOF structure along with flexibility in design and expert intelligence. The 2DOF FPI-D and 2DOF PI-D control schemes are also implemented for comparative study. The mathematical model of robotic manipulator discussed above is simulated in MATLAB to analyze the behavior of system. The simulations are performed on Intel®, CORE i3, 4 GB RAM, 1.70 GHz. personal computer using MATLAB software. Equation solver used for simulation is fourth-order Runge–Kutta with sampling time of $T = 1$ ms. Controlling torques τ_1 and τ_2 are restricted within the range $[-50, 50]$ Nm because of actuator limitation. The closed-loop control structure for considered manipulator has dedicated controller for each link. The performance of designed controllers for two-link robotic manipulator is rigorously examined by considering issues such as trajectory tracking, model uncertainties, disturbance and noise. The control scheme for 2DOF FOFPI-D is shown in Fig. 5.

5.1 Trajectory tracking performance

Robotic manipulators are used in industrial environment to perform various tasks such as pick and place, grinding and cutting. Links of the manipulator must follow a desired trajectory to perform a particular task. In this work, a cubic polynomial function of time is considered as desired trajectory for links [50]

$$\theta_{d_i}(t) = a_{0i} + a_{1i} t + a_{2i} t^2 + a_{3i} t^3 \tag{25}$$

where $\theta_{d_i}(t)$ is desired trajectory of link-1 and link-2 for $i = 1$ and 2, respectively. The boundary conditions for position of links are $\theta_{d_1} = 1$ rad and $\theta_{d_2} = 2$ rad at $t = 2$ s; $\theta_{d_1} = 0.5$ rad and $\theta_{d_2} = 4$ rad at $t = 4$ s. The corresponding angular velocities are $\dot{\theta}_{r_i} = 0$ rad/s at $t = 2$ and 4 s. The governing factors of NSGA-II for tuning the controllers are listed in Table 3. The search space for finding the optimum parameters of 2DOF FOFPI-D, its integer order counterpart and 2DOF PI-D is specified in Table 4. The value of filter coefficient N is considered to be '1000' for all controllers. Obtained Pareto front with chosen optimum solution for designed controllers is shown in Fig. 6, and corresponding optimum parameters, fitness and integral absolute error (IAE) are recorded in Table 5. The optimum parameters of controllers remain same for entire simulation studies.

The trajectory tracking performance of 2DOF FOFPI-D and other controllers in normal operating condition is shown in Fig. 7a, and the corresponding tracking error, controller effort and path traced by end-effector in rectangular (XY) coordinates are shown in Fig. 7b–d, respectively. It is observed from Table 5 that there is a significant improvement in IAE for 2DOF FOFPI-D over other controllers. The smaller value of IAE is due to incorporation of fractional order operator in the design, which provides the extra degrees of freedom to the controller. Also, the gains of controller are nonlinear function of input signals, which provide self-tuning control capability. Thus, 2DOF FOFPI-D controller tracks the trajectory more accurately as compared to other controllers. Further robustness of controllers is also tested for parametric uncertainties, actuator disturbance due to cogging and sensor noise in feedback path.

5.2 Model uncertainty

Mathematical modeling and identification of real-world robotic system are challenging issues as it is complex in nature and difficult to understand. Unavailability of exact mathematical model due to un-modeled dynamics, wear and tear and aging effect introduces uncertainty in the system. Therefore, an intelligent controller is required

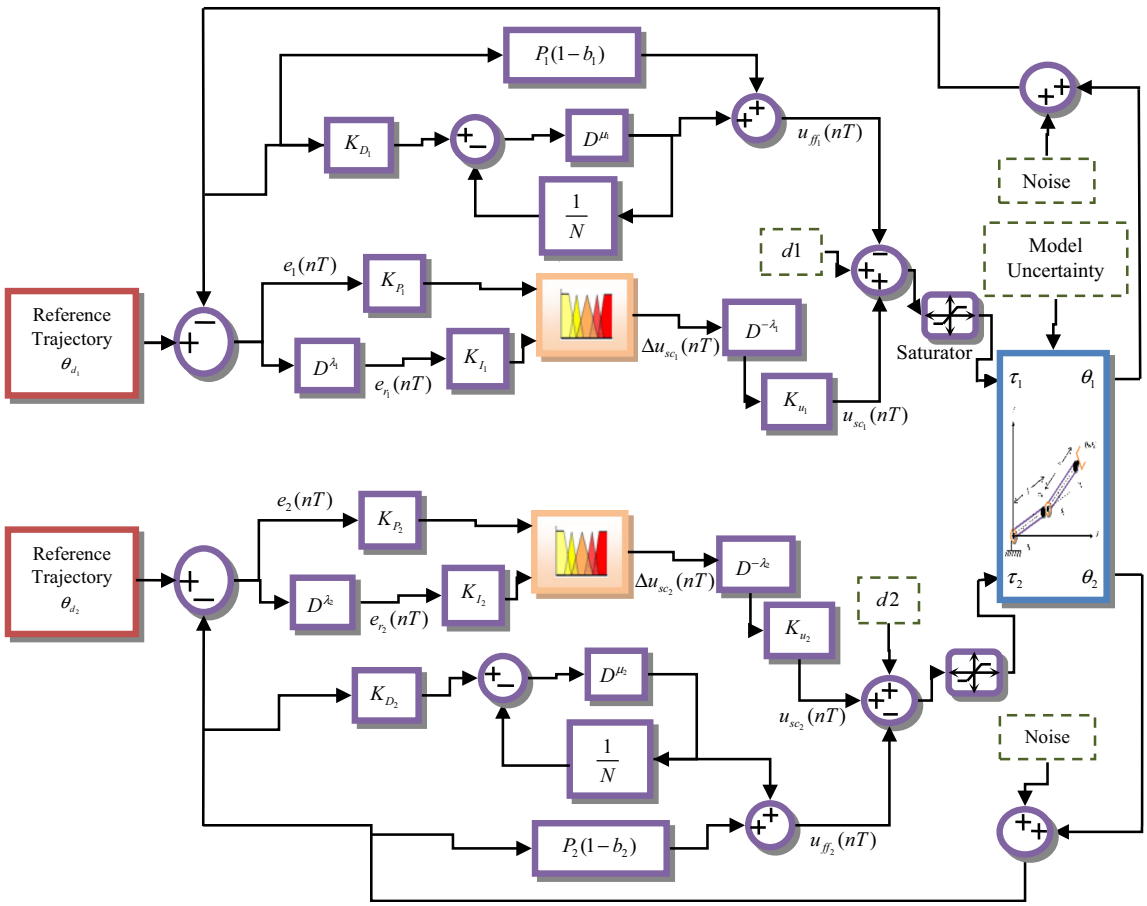

Fig. 5 Block diagram of 2DOF FOFPI-D control scheme for 2-link robotic manipulator

Table 3 NSGA-II parameters and their values for 2DOF FOFPI-D, 2DOF FPI-D and 2DOF PI-D controller

Parameter	Method and value for 2DOF FOFPI-D, 2DOF FPI-D, 2DOF FPI-D
Number of objective functions	2
Number of design variables	16, 12, 8
Population sizes	50
Maximum generation	200
Tournament pool size	2
Mutation method	Polynomial
Crossover method	Simulated binary crossover

which is capable enough to handle such uncertainties and provide satisfactory results. In this work, uncertainty in mass and length of both links is introduced in the model to evaluate the performance of designed controllers. The uncertain dynamics of manipulator is modeled by modifying Eqs. (23) and (24).

$$\begin{aligned}\tau_1 &= (m_2+\delta m_2)(l_2+\delta l_2)\Big((l_2+\delta l_2)(\ddot{\theta}_1+\ddot{\theta}_2)+g\cos(\theta_1+\theta_2)\Big)\\ &+(m_1+m_2+\delta m_1+\delta m_2)(l_1+\delta l_1)\Big((l_1+\delta l_1)\ddot{\theta}_1+g\cos\theta_1\Big)\\ &+(m_2+\delta m_2)(l_1+\delta l_1)(l_2+\delta l_2)\\ &\times\Big(\cos\theta_2(2\ddot{\theta}_1+\ddot{\theta}_2)-\sin\theta_2(\dot{\theta}_2^2)-2\sin\theta_2\dot{\theta}_1\dot{\theta}_2\Big)\end{aligned} \tag{26}$$

Table 4 Search range of parameters for various controllers

Controller parameters	2DOF FOFPI-D	2DOF FPI-D	2DOF PI-D
K_{P_i}, P_i and K_{D_i}	[0, 200]	[0, 200]	[0, 1000]
L_i and K_{u_i}	[0, 1000]	[0, 1000]	Not applicable
λ_i and μ_i	[0, 1]	1	1
b_i	[0, 1]	[0, 1]	[0, 1]

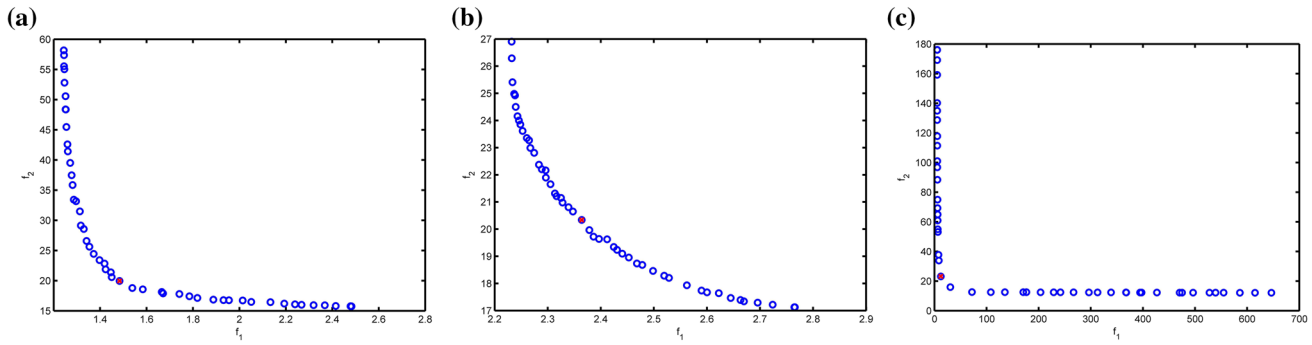

Fig. 6 Pareto front for objectives f_1 and f_2 using NSGA-II (**a**) 2DOF FOFPI-D (**b**) 2DOF FPI-D (**c**) 2DOF PI-D with chosen solution marked red

Table 5 Controller parameters, IAE and fitness functions of 2DOF FOFPI-D, 2DOF FPI-D and 2DOF PI-D controller for link-1 and link-2

Parameter link-1	2DOF FOFPI-D	2DOF FPI-D	2DOF PI-D	Parameter link-2	2DOF FOFPI-D	2DOF FPI-D	2DOF PI-D
P_1	16.1183	19.1461	980.564	P_2	4.9512	7.07487	880.722
K_{P_1}	195.987	155.732	872.362	K_{P_2}	190.113	138.571	711.235
K_{D_1}	25.1097	19.4326	4.57229	K_{D_2}	3.86684	2.77162	1.14507
K_{u_1}	897.091	598.405	–	K_{u_2}	549.105	500.226	–
L_1	731.775	715.723	–	L_2	89.1832	62.0572	–
b_1	0.616187	0.523962	0.9956	b_2	0.555904	0.41799	0.9997
λ_1	0.9785	1	1	λ_2	0.846896	1	1
μ_1	0.998829	1	1	μ_2	0.994847	1	1
IAE	$9.086 * 10^{-4}$	$14.09 * 10^{-4}$	$88.25 * 10^{-4}$	IAE	$5.748 * 10^{-4}$	$9.546 * 10^{-4}$	$33.33 * 10^{-4}$
f_1	**1.48363**	2.36401	12.1574				
f_2	**19.957**	20.3384	23.1651				

Bold values indicate the smallest value of objective functions for 2DOF FOFPI-D as compared to other designed controller

$$\tau_2 = (m_2 + \delta m_2)(l_1 + \delta l_1)(l_2 + \delta l_2)\left(\cos\theta_2\ddot{\theta}_1 + \sin\theta_2\dot{\theta}_1^2\right) + (m_2 + \delta m_2)(l_2 + \delta l_2)g\cos(\theta_1 + \theta_2) + (m_2 + \delta m_2)(l_2 + \delta l_2)^2\left(\ddot{\theta}_1 + \ddot{\theta}_2\right) \quad (27)$$

$$|\delta m_1| \leq \frac{d}{100} * m_1 \quad |\delta m_2| \leq \frac{d}{100} * m_2$$

$$|\delta l_1| \leq \frac{d}{100} * l_1 \quad |\delta l_2| \leq \frac{d}{100} * l_2$$

where δm_i and δl_i represents small change in mass and length, respectively, for ith link. d is the percentage uncertainty in system parameters.

Various cases of model uncertainty are considered by changing the value of 'd' from 5 to 30% with an interval of 5%. The designed controllers are employed to control the uncertain dynamics and the quantitative comparison is made on the basis of IAE value. The IAE of 2DOF FOFPI-D and other controllers for link-1 and link-2 are listed in Table 6, and the graphical representation is shown in Fig. 8. In all cases, IAE of 2DOF FOFPI-D controller for both links is smaller in contrast to other designed controllers, thereby proving its robustness against parametric uncertainty.

5.3 Disturbance rejection

The unforeseen disturbances arising in real-world systems are major concern for engineers, as they divert the output from its actual value. In robotic systems, disturbance emerges due to cogging and eccentricity of actuator, which produce low-frequency sinusoidal torque [53]. Subsequently, there is a necessity of a proficient controller, which is capable of dismissing such disturbances so that system response precisely tracks the reference.

The competency of designed control schemes is tested by adding sinusoidal disturbance for complete time duration and is represented by $d1$ and $d2$ in Fig. 5. Different cases are considered by changing the amplitude of disturbance from 1 to 10 Nm, and IAE of link-1 and link-2 for disturbance dismissal is recorded in Table 7. Disturbance rejection response for 10Sin25t Nm is depicted in Fig. 9, which comprises of trajectory tracking, error, control effort and path traced by end-effector in XY coordinates. It is clear from tabular and graphical investigation that IAE values of links are considerably smaller for 2DOF FOFPI-D controller as compared to 2DOF FPI-D and 2DOF PI-D

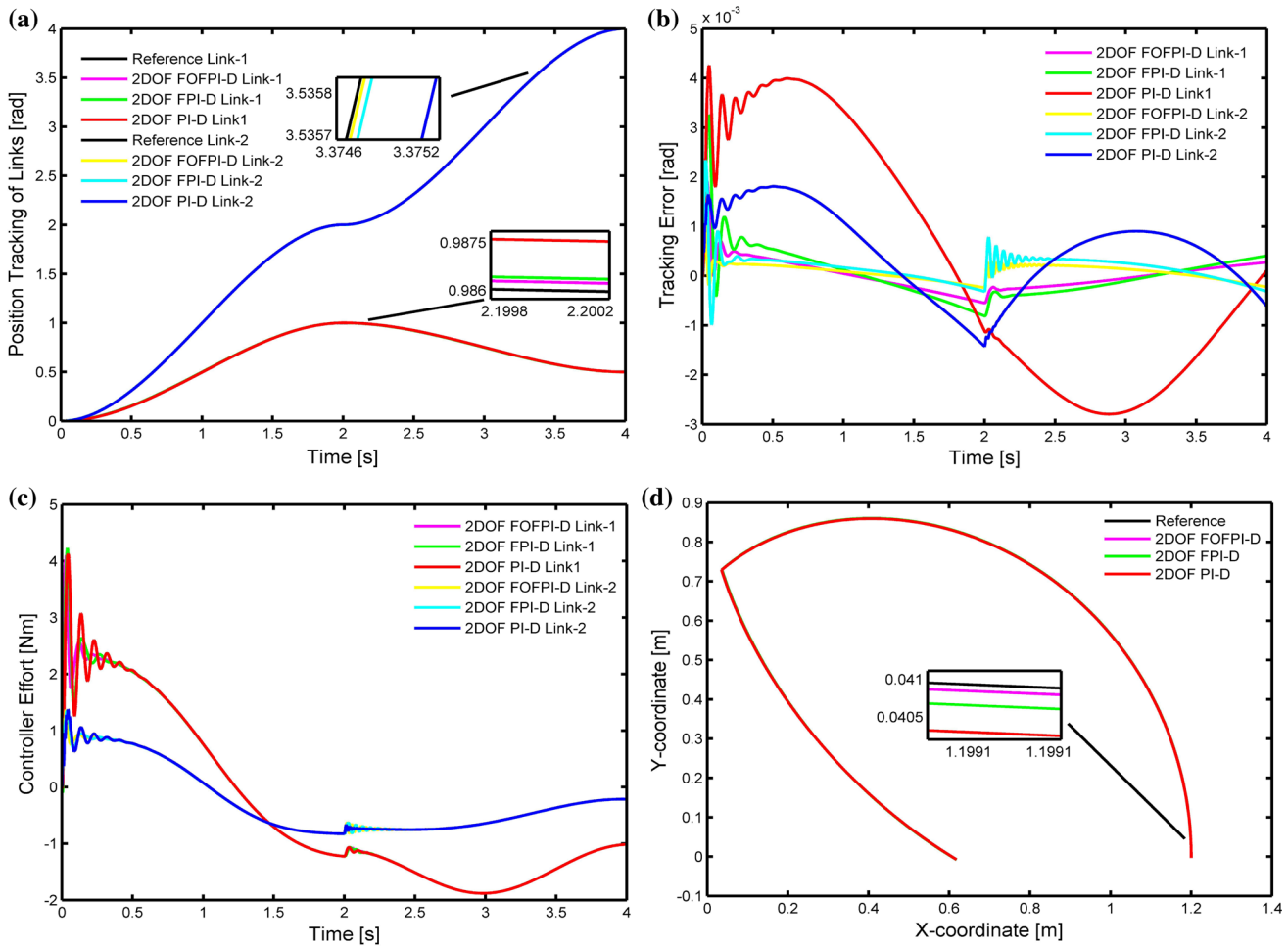

Fig. 7 Performance comparison of 2DOD FOFPI-D and other controllers: **a** reference trajectory tracking, **b** position error, **c** control effort, **d** path traced by end-effector in XY coordinates

Table 6 IAE values of various control schemes for $d\,\%$ uncertainty in m_1, m_2, l_1 and l_2

$d\,\%$ Uncertainty in m_1, m_2, l_1 and l_2	2DOF FOFPI-D		2DOF FPI-D		2DOF PI-D	
	link-1	link-2	link-1	link-2	link-1	link-2
5	0.0009091	0.0005784	0.001411	0.0009704	0.008815	0.003332
10	0.0009111	0.0006124	0.001413	0.001034	0.00879	0.003328
15	0.0009143	0.0006796	0.001414	0.001122	0.008751	0.003322
20	0.0009183	0.0007591	0.001415	0.001215	0.008698	0.003314
25	0.0009232	0.0008458	0.001414	0.001301	0.008632	0.003305
30	0.0009306	0.0009436	0.001414	0.001382	0.008554	0.003294

controller. Thus, disturbance rejection performance of 2DOF FOFPI-D is superior to other controllers.

5.4 Noise suppression

Practically real-time systems are predominantly affected by random noise due to inherent shortcomings of sensors, which deteriorates the output. A controller must be expert enough to conquer the impact of noise created in the system. The performance of controllers is examined by adding random noise to position of links as depicted in Fig. 5. Random noise of given maximum amplitude is generated and added to the position value (θ_1 and θ_2) in the simulation model. Different cases of random noise are considered by changing the maximum amplitude as given in Table 8. The IAE values of designed controllers for every

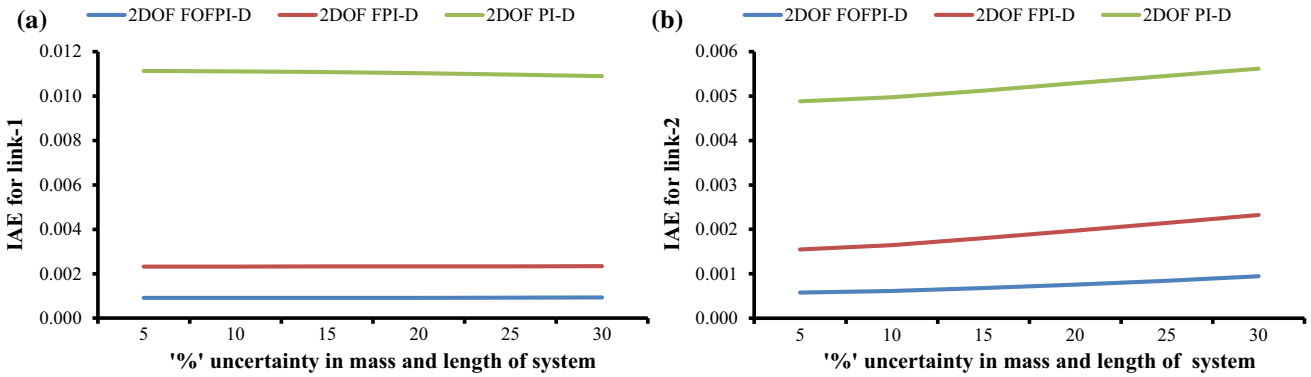

Fig. 8 Variation of IAE values for 2DOF FOFPI-D, 2DOF FPI-D and 2DOF PI-D with increasing % uncertainty in system parameters: **a** link 1 and **b** link 2

Table 7 IAE values of various controllers for added sinusoidal disturbance in $d1$ and $d2$

Disturbance in $\boldsymbol{d}1$ and $\boldsymbol{d}2$ (Nm)	2DOF FOFPI-D		2DOF FPI-D		2DOF PI-D	
	link-1	link-2	link-1	link-2	link-1	link-2
1Sin25t	0.001293	0.001095	0.002468	0.002659	0.009031	0.004115
2Sin25t	0.00214	0.002042	0.004436	0.005131	0.009718	0.006363
3Sin25t	0.00308	0.003021	0.006498	0.007643	0.01106	0.009123
4Sin25t	0.004043	0.00401	0.008594	0.01018	0.01311	0.01198
5Sin25t	0.005018	0.005004	0.01071	0.01271	0.01554	0.01488
6Sin25t	0.005999	0.005998	0.01283	0.01524	0.01811	0.01779
7Sin25t	0.006983	0.006994	0.01495	0.01777	0.02076	0.02071
8Sin25t	0.00797	0.007889	0.01708	0.0203	0.02346	0.02364
9Sin25t	0.008959	0.008984	0.01921	0.02282	0.02619	0.02658
10Sin25t	0.009949	0.009978	0.02134	0.02533	0.02894	0.02951

case of noise are also recorded in Table 8. The simulation results of 2DOF FOFPI-D and other controllers for trajectory tracking, position error, controller effort and movement of end-effector in XY coordinates for added 0.01 rad amplitude noise are shown in Fig. 10. It is implied from the analysis that IAE values of 2DOF FOFPI-D controller are smaller as compared to 2DOF FPI-D and conventional 2DOF PI-D controller for all instances of noise. Hence, it is concluded that 2DOF FOFPI-D scheme suppresses the noise most efficiently in comparison with other controllers.

5.5 Simultaneous uncertainty, noise and disturbance rejection

The performance of controllers is investigated by simultaneously incorporating model uncertainties, sensor noise as well as disturbance in the system. The entire study is performed by taking 30% model uncertainty, sensor noise of 0.01 rad in links, disturbance of 10Sin25t Nm and desired trajectory for link-1 and link-2 as

$$\theta_{d_1}(t) = 5.3678 - 5.3678 * \cos(1.567t) \quad (28)$$

$$\theta_{d_2}(t) = 3.8126 * \cos(2.138t) - 3.8126 \quad (29)$$

The trajectory tracking performance of designed controllers and their corresponding tracking error, torque and path traced by end-effector in rectangular coordinates are shown in Fig. 11. Further, the quantitative assessment of controllers on the basis of IAE is depicted in Fig. 12. It is found that IAE of 2DOF FPI-D and 2DOF PI-D for link-1 are approximately 1.26 and 3.68 times the IAE of 2DOF FOFPI-D controller, respectively. For link-2, they are 1.12 and 1.53 times the IAE of 2DOF FOFPI-D controller, respectively. Thus, IAE values of 2DOF FOFPI-D for both links are smallest among designed controllers. 2DOF FOFPI-D controller hence proves to be more robust and superior to its integer order counterpart and 2DOF PI-D controller.

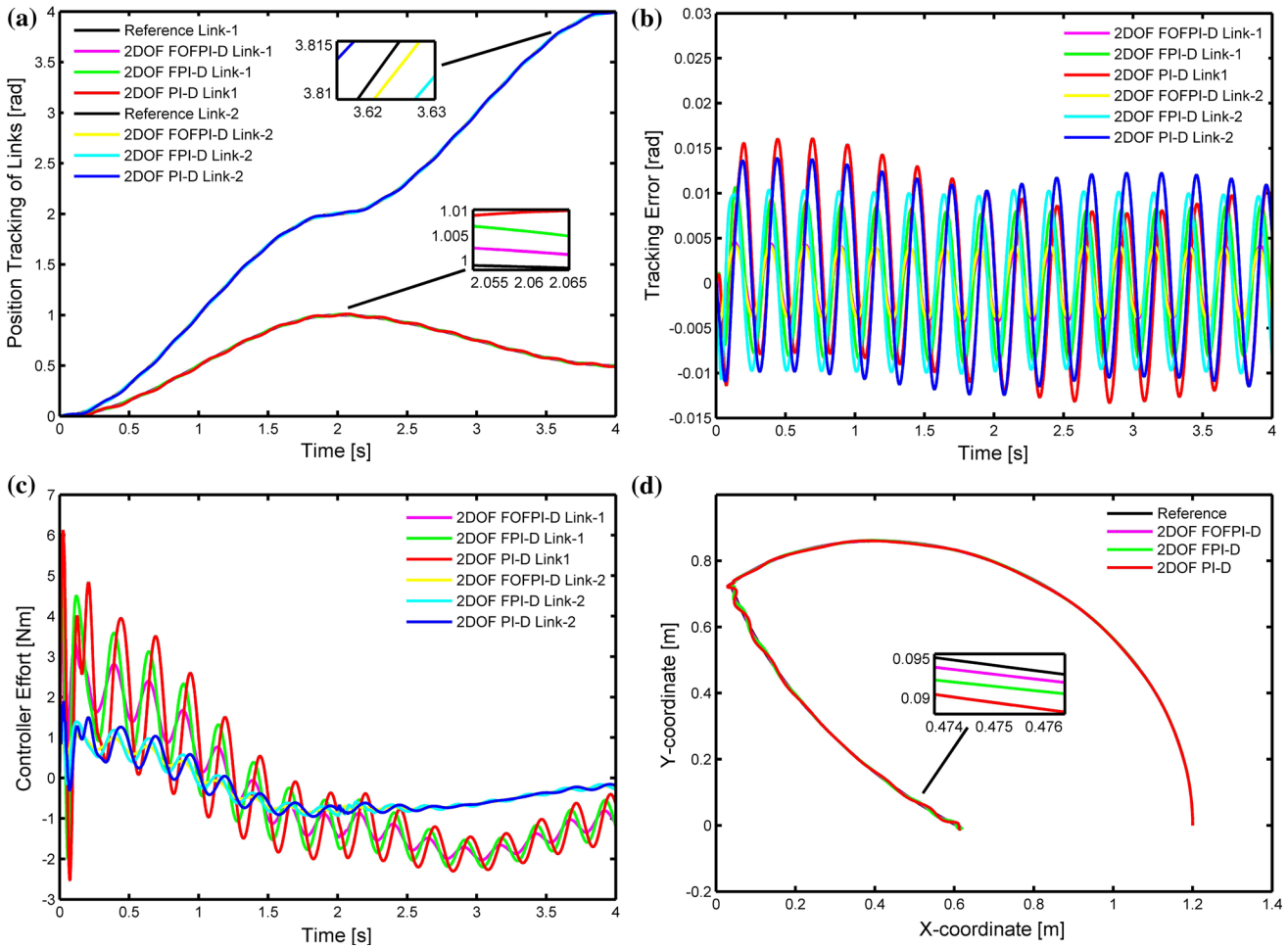

Fig. 9 Performance comparison of designed controllers: **a** trajectory tracking, **b** position error, **c** control effort, **d** movement of end-effector in rectangular coordinates by adding 10Sin25t Nm disturbance in $d1$ and $d2$

Table 8 IAE value of various controllers for added random noise

Maximum amplitude of noise (rad)	2DOF FOFPI-D		2DOF FPI-D		2DOF PI-D	
	link-1	link-2	link-1	link-2	link-1	link-2
0.002	0.01042	0.0109	0.02139	0.02524	0.02919	0.02977
0.004	0.01227	0.01366	0.02198	0.02571	0.02977	0.03047
0.006	0.01561	0.01783	0.0235	0.027	0.03077	0.03174
0.008	0.01973	0.02276	0.02607	0.02922	0.03225	0.03374
0.01	0.02446	0.02859	0.02958	0.03221	0.03421	0.03645

6 Discussion

In real-time robotic manipulator, the actuator may experience disturbance due to locking of the rotor at specific points. These disturbances are sinusoidal in nature and arise due to the phenomenon of cogging and eccentricity [53]. Also high-frequency noise in the feedback sensor degrades the performance of system. Inherent shortcomings, design and aging effect are the main cause of sensor noise. Another issue with real-time system is frequent change in reference and uncertain dynamics. To evaluate the capability of designed controllers in dealing with such adverse conditions, a real-time environment is virtually created in MATLAB.

The designed controllers are implemented in discrete-time domain; therefore, sampling time 'T' becomes an important parameter. The value of T needs to be selected in such a way that enough number of samples are obtained for analysis. If sampling time is too large, the signal information is lost and retrieved response is distorted. If

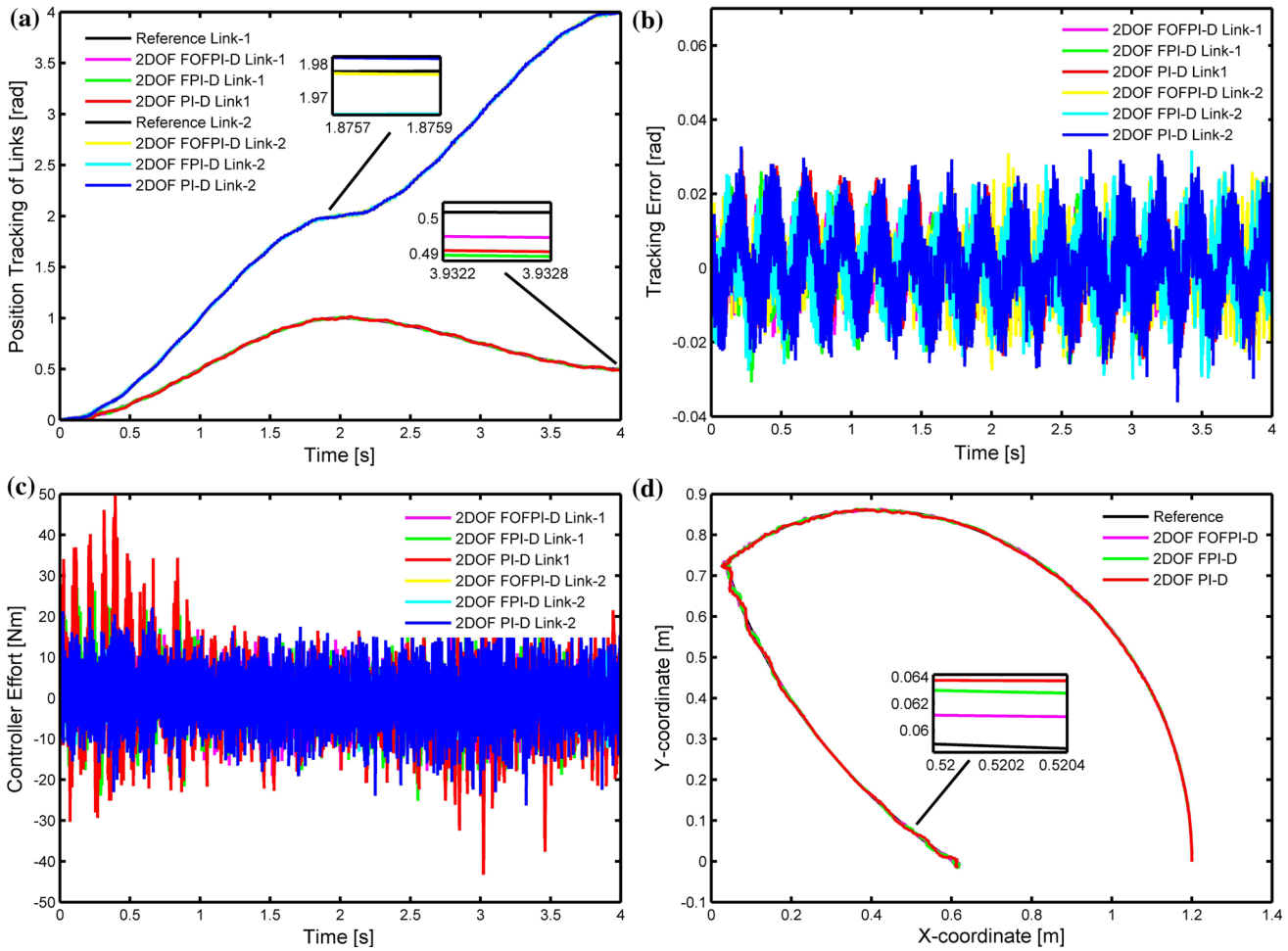

Fig. 10 Performance comparison of designed controllers: **a** trajectory tracking, **b** position error, **c** control effort, **d** tracking of end-effector in rectangular coordinates by adding 0.01 rad noise in links

sampling time is too small, large number of redundant samples will be generated which increases simulation time [32]. Thus, sampling time directly affects the system performance and it should be selected appropriately. The value of sampling time 'T' is taken as 0.001 s. Further total time taken by NSGA-II algorithm to generate Pareto front for 200th generation in case of 2DOF FOFPI-D is 22,167.9 s, for 2DOF FPI-D is 20,143.2 s, whereas for 2DOF PI-D is 16,884.3 s. The time taken to tune 2DOF FOFPI-D is larger because of additional design variables due to fractional order operators. This increases the computational complexity during optimization of controller parameters. The time taken to optimize also depends on the sampling time. However, the complexity in controller does not affect the time taken to obtain the controlled variable. All the designed controllers take almost same time to generate the control signal.

The control objectives for robotic manipulator are precise position tracking with minimum variation in control signal. A 2DOF PI-D controller has the capability to handle several requirements, which makes it suitable for the task at hand. The PI compensator and derivative filter components of the controller are tuned compatibly to achieve the desired objectives. Thus, IAE values are quite low for links 1 and 2, i.e., $88.25 * 10^{-4}$ and $33.33 * 10^{-4}$, respectively. Further the controller performance remains consistent under model uncertainties, but disturbance and noise degrade the controller performance. So to improve the performance of 2DOF PI-D controller, fuzzy expertise is embedded in PI compensator, which leads to 2DOF FPI-D. The designed controller further reduces the values of IAE as compared to 2DOF PI-D for tracking response under the influence of disturbance and noise. The controller provides good performance for introduction of parametric uncertainty with 30% as maximum change in the system parameters. This is due to the reason that formula-based fuzzy design scheme is not model specific, possesses self-tuning ability and requires only experience-based knowledge about operation of the system. The performance of controller is further enhanced by providing flexibility in

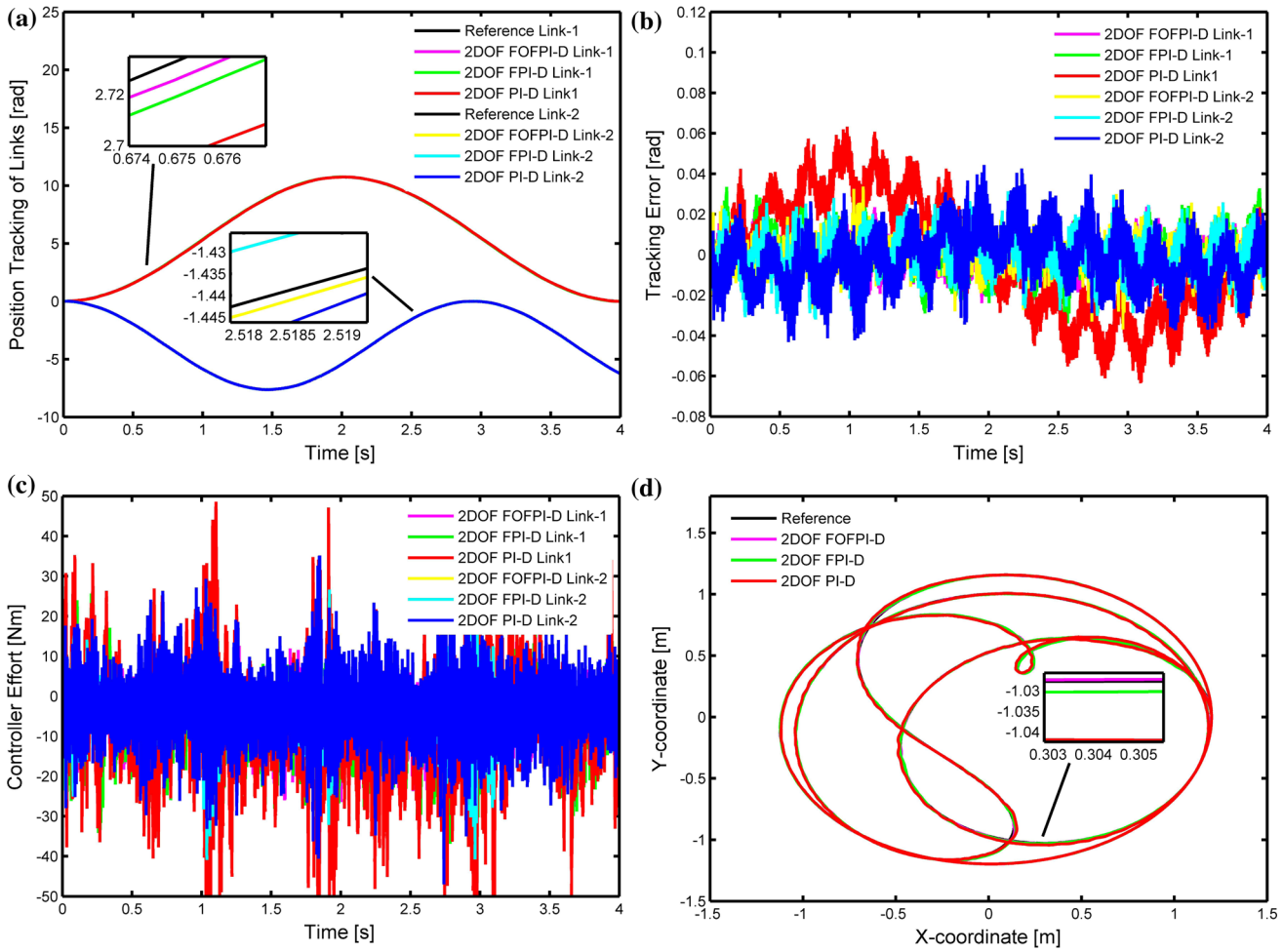

Fig. 11 Performance comparison of designed controllers for 30% parameter uncertainties, disturbance of 10Sin25*t* Nm and random noise of 0.01 rad to links: **a** trajectory tracking, **b** position error, **c** control effort, **d** movement of end-effector in rectangular coordinate

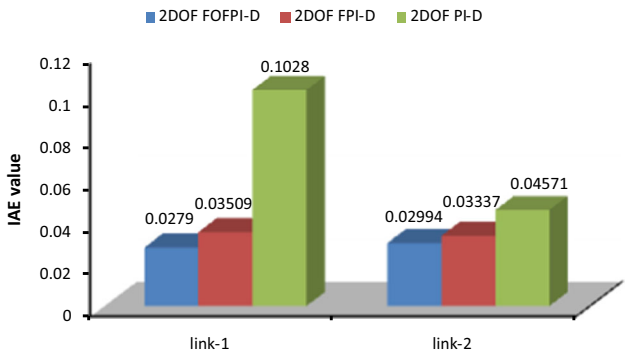

Fig. 12 Quantitative comparison of various controllers for link-1 and link-2 by incorporating 30% parameter uncertainties, disturbance of 10Sin25*t* Nm and random noise of amplitude 0.01 rad to links

design by inclusion of fractional order operator, which leads to 2DOF FOFPI-D control strategy. The results acquired for tracking control, uncertain parameters, disturbance rejection and noise suppression have lowest value of IAE, and accurate tracking is achieved. The only limitation of proposed controller is increased number of design variables due to incorporation of fractional order operators. The tuning of increased variables becomes a combinatorial problem; however, this issue may be overcome by optimization of controller parameters.

7 Concluding remarks

In this paper, a generic 2DOF FOFPI-D for control of nonlinear systems is presented. The proposed controller is a combination of serial compensator (FOFPI) and fractional order derivative filter (FODF), which is derived from traditional 2DOF FOPID. Analytical formulae for control law and implementation of fuzzy logic are derived to support the structure of controller. 2DOF FPI-D and 2DOF PI-D controllers are also designed for comparative study. A coupled, nonlinear two-link robotic manipulator is considered to evaluate the performance of designed controllers. The manipulator model replicates the real

operating environment of system by considering multiple issues such as parametric uncertainty, presence of disturbance due to cogging and noise generated by sensors. The objective of the controller is to provide accurate tracking in the presence of noise and disturbance with constraints that variation in control signal is minimal. It is revealed from the results that 2DOF FOFPI-D controller efficiently handles multiple issues, due to increased degrees of freedom, fuzzy logic expertise and flexibility of fractional operator in comparison with other designed controllers. Future work may be focused toward establishing the analytical stability conditions and its real-time implementation [2, 31]. Further applicability of designed controllers to complex systems with essential nonlinearities, particularly servo system, fractional order dynamic systems, and chaotic system may also be analyzed.

Compliance with ethical standards

Conflict of interest All authors declare that he/she has no conflict of interest.

Ethical approval This article does not contain any studies with human participants or animals performed by any of the authors.

References

1. Miccio M, Cosenza B (2014) Control of a distillation column by type-2 and type-1 fuzzy logic PID controllers. J Process Control 24(5):475–484
2. Precup R-E, Preitl S, Petriu EM, Tar JK, Tomescu ML, Pozna C (2009) Generic two-degree-of-freedom linear and fuzzy controllers for integral processes. J Frankl Inst 346(10):980–1003
3. Malki HA, Li H, Chen G (1994) New design and stability analysis of fuzzy proportional-derivative control systems. IEEE Trans Fuzzy Syst 2(4):245–254
4. Misir D, Malki HA, Guanrong C (1996) Design and analysis of a fuzzy proportional–integral–derivative controller. Fuzzy Sets Syst 79(3):297–314
5. Malki HA, Misir D, Feigenspan D, Guanrong C (1997) Fuzzy PID control of a flexible-joint robot arm with uncertainties from time-varying loads. IEEE Trans Control Syst Technol 5(3):371–378
6. Sooraksa P, Chen G (1998) Mathematical modeling and fuzzy control of a flexible-link robot arm. Math Comput Model 27(6):73–93
7. Li W, Chang X, Wahl FM, Farrell J (2001) Tracking control of a manipulator under uncertainty by FUZZY P + ID controller. Fuzzy Sets Syst 122(1):125–137
8. Er MJ, Sun YL (2001) Hybrid fuzzy proportional-integral plus conventional derivative control of linear and nonlinear systems. IEEE Trans Ind Electron 48(6):1109–1117
9. Tang KS, Kim Fung M, Guanrong C, Kwong S (2001) An optimal fuzzy PID controller. IEEE Trans Ind Electron 48(4):757–765
10. Tang W, Chen G, Lu R (2001) A modified fuzzy PI controller for a flexible-joint robot arm with uncertainties. Fuzzy Sets Syst 118(1):109–119
11. Ying H, Siler W, Buckley JJ (1990) Fuzzy control theory: a nonlinear case. Automatica 26(3):513–520
12. Chen G, Pham TT (2000) Introduction to fuzzy sets, fuzzy logic, and fuzzy control systems. CRC Press, Boca Raton
13. Mohan V, Rani A, Singh V (2017) Robust adaptive fuzzy controller applied to double inverted pendulum. J Intell Fuzzy Syst 32(5):3669–3687
14. Kumar A, Kumar V (2017) Hybridized ABC-GA optimized fractional order fuzzy pre-compensated FOPID control design for 2-DOF robot manipulator. AEU Int J Electron Commun 79(Supplement C):219–233
15. Kumar A, Kumar V (2018) Performance analysis of optimal hybrid novel interval type-2 fractional order fuzzy logic controllers for fractional order systems. Expert Syst Appl 93(Supplement C):435–455
16. Sharma R, Gaur P, Mittal A (2016) Design of two-layered fractional order fuzzy logic controllers applied to robotic manipulator with variable payload. Appl Soft Comput 47:565–576
17. Das S, Pan I, Das S (2013) Performance comparison of optimal fractional order hybrid fuzzy PID controllers for handling oscillatory fractional order processes with dead time. ISA Trans 52(4):550–566
18. Das S, Pan I, Das S, Gupta A (2012) A novel fractional order fuzzy PID controller and its optimal time domain tuning based on integral performance indices. Eng Appl Artif Intell 25(2):430–442
19. Kumar V, Rana KPS, Kumar J, Mishra P (2016) Self-tuned robust fractional order fuzzy PD controller for uncertain and nonlinear active suspension system. Neural Comput Appl. https://doi.org/10.1007/s00521-016-2774-x
20. Jesus IS, Barbosa RS (2015) Genetic optimization of fuzzy fractional PD + I controllers. ISA Trans 57:220–230
21. Haji VH, Monje CA (2017) Fractional order fuzzy-PID control of a combined cycle power plant using Particle Swarm Optimization algorithm with an improved dynamic parameters selection. Appl Soft Comput 58:256–264
22. Zamani A-A, Tavakoli S, Etedali S, Sadeghi J (2017) Adaptive fractional order fuzzy proportional–integral–derivative control of smart base-isolated structures equipped with magnetorheological dampers. J Intell Mater Syst Struct. https://doi.org/10.1177/1045389X17721046
23. Pan I, Korre A, Das S, Durucan S (2012) Chaos suppression in a fractional order financial system using intelligent regrouping PSO based fractional fuzzy control policy in the presence of fractional Gaussian noise. Nonlinear Dyn 70(4):2445–2461
24. Pan I, Das S (2016) Fractional order fuzzy control of hybrid power system with renewable generation using chaotic PSO. ISA Trans 62:19–29
25. Sharma R, Rana KPS, Kumar V (2014) Performance analysis of fractional order fuzzy PID controllers applied to a robotic manipulator. Expert Syst Appl 41(9):4274–4289
26. Kumar V, Rana K (2017) Nonlinear adaptive fractional order fuzzy PID control of a 2-link planar rigid manipulator with payload. J Frankl Inst 354(2):993–1022
27. Das S, Pan I, Das S (2013) Fractional order fuzzy control of nuclear reactor power with thermal-hydraulic effects in the presence of random network induced delay and sensor noise having long range dependence. Energy Convers Manag 68:200–218
28. Mishra P, Kumar V, Rana K (2015) A fractional order fuzzy PID controller for binary distillation column control. Expert Syst Appl 42(22):8533–8549
29. Kumar V, Rana K, Mishra P (2016) Robust speed control of hybrid electric vehicle using fractional order fuzzy PD and PI controllers in cascade control loop. J Frankl Inst 353(8):1713–1741

30. Araki M, Taguchi H (2003) Two-degree-of-freedom PID controllers. Int J Control Autom Syst 1:401–411
31. Sharma R, Gaur P, Mittal A (2015) Performance analysis of two-degree of freedom fractional order PID controllers for robotic manipulator with payload. ISA Trans 58:279–291
32. Pachauri N, Singh V, Rani A (2017) Two degree of freedom PID based inferential control of continuous bioreactor for ethanol production. ISA Trans 68:235
33. Ghosh A, Rakesh Krishnan T, Tejaswy P, Mandal A, Pradhan JK, Ranasingh S (2014) Design and implementation of a 2-DOF PID compensation for magnetic levitation systems. ISA Trans 53(4):1216–1222
34. Debbarma S, Saikia LC, Sinha N (2014) Automatic generation control using two degree of freedom fractional order PID controller. Int J Electr Power Energy Syst 58:120–129
35. Li M, Zhou P, Zhao Z, Zhang J (2016) Two-degree-of-freedom fractional order-PID controllers design for fractional order processes with dead-time. ISA Trans 61:147–154
36. Deb K, Pratap A, Agarwal S, Meyarivan T (2002) A fast and elitist multiobjective genetic algorithm: NSGA-II. IEEE Trans Evol Comput 6(2):182–197
37. Kumar V, Rana K (2016) Some investigations on hybrid fuzzy IPD controllers for proportional and derivative kick suppression. Int J Autom Comput 13(5):516–528
38. Lipták BG (2013) Process control: instrument engineers' handbook. Butterworth-Heinemann, Oxford
39. Gopal M (2002) Control systems: principles and design. Tata McGraw-Hill Education, New York
40. Goodrich C, Peterson AC (2016) Discrete fractional calculus. Springer, Berlin
41. Lubich C (1986) Discretized fractional calculus. SIAM J Math Anal 17(3):704–719
42. Zadeh LA (1965) Fuzzy sets. Inf Control 8(3):338–353
43. Kumar S, Saxena R, Singh K (2017) Fractional Fourier transform and fractional-order calculus-based image edge detection. Circuits Syst Signal Process 36(4):1493–1513
44. Tsirimokou G, Psychalinos C, Elwakil A (2017) Current-mode fractional-order filters. In: Gan W-S, Kuo C-CJ, Zheng ThF, Barni M (eds) Design of CMOS analog integrated fractional-order circuits. SpringerBriefs in electrical and computer engineering. Springer, Berlin, pp 41–54
45. Oldham K, Spanier J (1974) The fractional calculus theory and applications of differentiation and integration to arbitrary order. Elsevier, Amsterdam
46. Chen Y, Petras I, Xue D (2009) Fractional order control-a tutorial. pp 1397–1411. https://doi.org/10.1109/ACC.2009.5160719
47. Podlubny I (1998) Fractional differential equations: an introduction to fractional derivatives, fractional differential equations, to methods of their solution and some of their applications. Academic Press, Cambridge
48. Pan I, Das S (2012) Chaotic multi-objective optimization based design of fractional order $PI\lambda D^{\mu}$ controller in AVR system. Int J Electr Power Energy Syst 43(1):393–407
49. Chen Z, Yuan X, Ji B, Wang P, Tian H (2014) Design of a fractional order PID controller for hydraulic turbine regulating system using chaotic non-dominated sorting genetic algorithm II. Energy Convers Manag 84:390–404
50. Ayala HVH, dos Santos Coelho L (2012) Tuning of PID controller based on a multiobjective genetic algorithm applied to a robotic manipulator. Expert Syst Appl 39(10):8968–8974
51. Esfe MH, Razi P, Hajmohammad MH, Rostamian SH, Sarsam WS, Arani AAA, Dahari M (2017) Optimization, modeling and accurate prediction of thermal conductivity and dynamic viscosity of stabilized ethylene glycol and water mixture Al_2O_3 nanofluids by NSGA-II using ANN. Int Commun Heat Mass Trans 82:154–160
52. Craig JJ (2005) Introduction to robotics: mechanics and control. Pearson Prentice Hall, Upper Saddle River
53. De Wit CC, Praly L (2000) Adaptive eccentricity compensation. IEEE Trans Control Syst Technol 8(5):757–766